Environmental Fluid Mechanics **1:** 209–233, 2001.

Numerical Investigation of the Effects of Boundary-Layer Evolution on the Predictions of Ozone and the Efficacy of Emission Control Options in the Northeastern United States

JIA-YEONG KU[a], HUITING MAO[b], KESU ZHANG[b], KEVIN CIVEROLO[a], S. TRIVIKRAMA RAO[a,b,*], C. RUSSELL PHILBRICK[c], BRUCE DODDRIDGE[d] and RICHARD CLARK[e]

[a]*New York State Department of Environmental Conservation, Albany, NY 12233–3259, U.S.A.*
[b]*University at Albany, Department of Earth and Atmospheric Sciences, Albany, NY 12222, U.S.A.*
[c]*Pennsylvania State University, Department of Electrical Engineering, University Park, PA 16802, U.S.A.*
[d]*University of Maryland, Department of Meteorology, College Park, MD 20742, U.S.A.*
[e]*Millersville University, Department of Earth Sciences, Millersville, PA 17551, U.S.A.*

Received 2 February 2001; accepted in revised form 5 April 2001

Abstract. This paper examines the effects of two different planetary boundary-layer (PBL) parameterization schemes – Blackadar and Gayno–Seaman – on the predicted ozone (O_3) concentration fields using the MM5 (Version 3.3) meteorological model and the MODELS-3 photochemical model. The meteorological fields obtained from the two boundary-layer schemes have been used to drive the photochemical model to simulate O_3 concentrations in the northeastern United States for a three-day O_3 episodic period. In addition to large differences in the predicted O_3 levels at individual grid cells, the simulated daily maximum 1-h O_3 concentrations appear at different regions of the modeling domain in these simulations, due to the differences in the vertical exchange formulations in these two PBL schemes. Using process analysis, we compared the differences between the different simulations in terms of the relative importance of chemical and physical processes to O_3 formation and destruction over the diurnal cycle. Finally, examination of the photochemical model's response to reductions in emissions reveals that the choice of equally valid boundary-layer parameterizations can significantly influence the efficacy of emission control strategies.

Key words: mixing heights, ozone, photochemical models, planetary boundary-layer

1. Introduction

An air quality modeling system consists of a meteorological model, an emissions processing model, and a photochemical model. It is well known that the ability of any grid-based photochemical model to reproduce the observed ozone (O_3) concentrations depends to a large extent on the accuracy of the meteorological fields used as model inputs [1–4]. The uncertainties in the air quality modeling system may arise from initial conditions [5], representativeness of the physical and chem-

*Corresponding author, E-mail: strao@dec.state.ny.us

ical processes, boundary conditions, and inaccuracies in the emissions inventory [6]. The planetary boundary-layer (PBL) processes included in the meteorological models dictate the temporal evolution and depth of the mixed-layer, intensity of the turbulent mixing, and accuracy of the wind fields [7]. Because different PBL schemes rely upon different parameterizations and emphasize different physical processes, it is not surprising that the use of different PBL schemes can yield very different vertical profiles of simulated parameters, including temperature, water vapor mixing ratio, and horizontal winds, particularly during the daytime growth of the mixed-layer [8–10]. These parameters exert a strong influence on the formation, spatial distribution, and removal of airborne chemical species in the atmosphere [11, 12].

In the photochemical model simulations, three important boundary-layer parameters for studying air pollution events are the mixing height, ventilation coefficient, and cloud cover [7]. The mixing height is the depth, measured upward from the earth's surface, through which air pollutants are mixed. The ventilation coefficient is defined as the product of the mixing height and average wind speed within the mixed layer. Large ventilation coefficients suggest increased dilution, leading to lower pollutant concentration levels. In a study of the summertime conditions over the northeastern United States, Berman *et al.* [9] showed that average ventilation coefficients during early morning hours in the Northeast were approximately 50% lower on O_3 episode days than on non-episode days. Clouds and precipitation scavenge pollutants from the air. Clouds can also affect gas-phase chemistry by attenuating solar radiation below the cloud base, having a significant impact on the photolytic reactions.

Previous studies indicated that O_3 concentrations simulated by the Urban Airshed Model (UAM-IV) are sensitive to errors and uncertainties in the specification of the mixing-height profile [13]. Also, the selection of appropriate pollution control strategies seemed to depend on the spatial and temporal variability of the mixing height over the modeling domain [14].

In this study, meteorological fields were simulated with the Fifth Generation Penn State-NCAR Mesoscale Model (MM5, Version 3.3) [15], a three-dimensional non-hydrostatic prognostic model, for a high O_3 episode that occurred over the northeastern United States during July 12-17, 1999. We employed two different boundary-layer schemes for the MM5 simulations: the hybrid local and non-local closure scheme proposed by Blackadar [16], and the 1.5-order turbulent kinetic energy (TKE) closure scheme developed by Gayno *et al.* [17]. Zhang *et al.* [10] described the MM5 simulations performed with these two PBL schemes and discussed the differences in the meteorological fields, including winds, temperature, and water vapor for the July 12–17, 1999 period. In this analysis, we used these MM5 fields as input to the U.S. Environmental Protection Agency's (EPA) MODELS-3 Community Multiscale Air Quality model (CMAQ) [18], for the July 12–17 period. These simulations were carried out in support of the North American Research Strategy on Tropospheric Ozone's NorthEast-Oxidant and Particle Study

(NARSTO-NE-OPS) campaign [19], an intensive monitoring program located at the Baxter Water Treatment Plant in Philadelphia, PA, hereafter referred to as the 'Baxter site'.

The objectives of this paper are to examine the effects of the different PBL schemes, as well as the effects of different PBL height diagnosis by different methods on the simulated meteorological and O_3 fields, and to characterize the associated modeling uncertainties. In addition to examining the model's response to different meteorological inputs, we assess the sensitivity of the O_3 predictions to the emission reductions which result from the different PBL schemes.

2. Methods of Analysis

2.1. METEOROLOGICAL MODELING SYSTEM (MM5)

We performed two sets of meteorological modeling simulations with MM5 Version 3.3 [15] for the July 12–17, 1999 period using two different PBL schemes – the Blackadar scheme [16, 20] and the Gayno–Seaman scheme [17]. The details of these two simulations and the modeling results can be found in Zhang *et al.* [10]. Briefly, during the convective conditions, the non-local mixing of the Blackadar PBL scheme assumes that buoyant plumes from the surface rise and mix across all layers over the boundary-layer, exchanging momentum, energy, moisture, and other scalar quantities. The intensity of mixing, defined as the fraction of mass exchanged between the surface layer and the other layers within the PBL, is based on the surface heat flux. The result is that these parameters are distributed uniformly throughout the boundary-layer within a short period of time. The local mixing of the Gayno–Seaman PBL scheme calculates TKE prognostically. The vertical diffusion coefficient (K_v) is then diagnosed based on the local value of TKE. The scheme may not be simply regarded as a local scheme, since TKE may be generated elsewhere in the domain and transported to the local grid cell. The Blackadar scheme differs from Gayno–Seaman scheme in that the latter mixes scalars only between two adjacent layers at a time, while the former mixes across all layers simultaneously under convective conditions. Hereafter, the two PBL schemes will be referred to as 'BL' and 'GS', respectively.

2.2. PHOTOCHEMICAL MODELING SYSTEM (CMAQ/MODELS-3)

The CMAQ is a three-dimensional photochemical model of the EPA's MODELS-3 system. The CMAQ's 12 km horizontal grid structure follows that of MM5, consisting of 163 cells along the east-west direction and 145 cells along the north-south direction, covering a large portion of the eastern United States. Figure 1 displays the modeling domain and the northeastern U.S. analysis subdomain. There are 16 layers in the vertical, with the first 12 layers (below 3124 m) identical to that of MM5 to maintain high resolution within the PBL [10]. Note, the vertical diffusion of CMAQ is based on the K-theory scheme which is different from MM5's

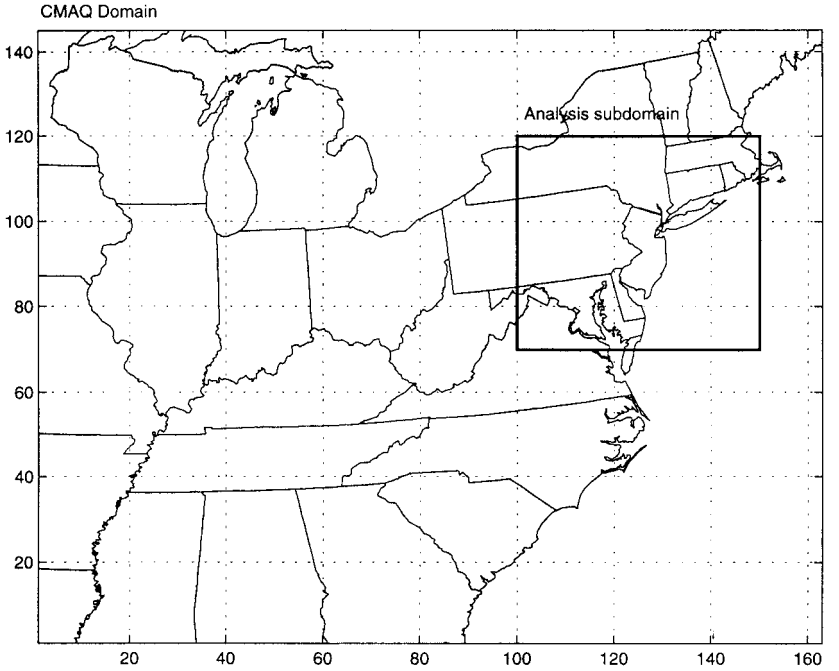

Figure 1. The 12 km modeling domain and the northeastern U.S. analysis subdomain in MODELS-3.

approaches. For the convective boundary-layer, the eddy diffusivity is defined as a function of surface convective velocity and PBL height. The Carbon Bond IV (CB4) [21] chemical mechanism is used in the CMAQ simulations. Since a gridded emissions inventory was not available for the July 1999 period, we used the emissions inventory reported by Sistla *et al.* [3], for the mid-July 1995 period in this study. Since the primary objective of this study is to examine the uncertainty caused by the meteorological inputs, the same emissions were used all base case simulations.

In order to assess the relative contributions of different physical and chemical processes, we performed process analysis (PA) for each of the CMAQ simulations. The process analysis feature of CMAQ allows the user to compare the relative contributions of vertical diffusion, horizontal advection, in-situ chemical production, and other processes relative to the formation or destruction of O_3 at each grid cell as a function of time. Thus, we can cross-compare the magnitudes and the diurnal variations of the contributions of these processes to the predicted O_3 formation rates.

Since photochemical models are being widely used as tools to guide regulatory decisions, it is important to determine how the meteorological uncertainty propagating into the photochemical model affects the simulations of O_3 under different emission control scenarios. Therefore, we investigated the response of

the predicted O_3 concentrations to different hypothetical anthropogenic emissions reduction scenarios using the different meteorological inputs. We created two additional sets of gridded emissions which incorporated spatially uniform reductions in nitrogen oxides (NO_x) and volatile organic compounds (VOC) emissions from the base case; one of the emissions reduction scenarios is more NO_x-focused (i.e., NO_xreduced by 50%, and VOC reduced by 25%; hereafter referred to as N50V25), while the other is more VOC-focused (i.e., 25% reduction in NO_x, and 50% reduction in VOC; hereafter referred to as N25V50). Additional CMAQ simulations were performed with these two sets of emissions reduction cases, and the effects of emission changes on predicted O_3 levels for the two sets of meteorological fields are examined here.

2.3. EXPERIMENTAL DESIGN OF THE BASE CASE SIMULATIONS

In this study, the differences between the various meteorological and photochemical simulations are solely due to differences in the PBL schemes and the methods for diagnosing the PBL height by MM5 and MODELS-3. In MM5, the convective PBL height diagnosis depends on the PBL scheme used; the BL scheme relies on the buoyant energy (θ-profile), while the GS scheme defines the PBL height either at the level where the TKE has fallen to 0.1 $m^2\ s^{-2}$ in the case of strong convection (maximum TKE $> 0.2\ m^2\ s^{-2}$), or 50% of the maximum TKE in the case of weak convection (maximum TKE $< 0.2\ m^2\ s^{-2}$) [22]. On the other hand, the MODELS-3 preprocessor defines the PBL height as the level where the bulk Richardson number reaches a maximum of 0.7, regardless of the PBL scheme in the meteorological model [18]. Therefore, the MODELS-3 pre-processor re-diagnoses the PBL height, creating a potential dynamical inconsistency with the meteorological fields.

In this analysis, four base case photochemical simulations have been performed. The purpose of the four simulations is to investigate the sensitivity of the CMAQ simulations to the differences of PBL schemes and PBL height diagnosis, keeping the input emissions unchanged. After the MM5 meteorological fields are generated with the two PBL schemes, they are processed to create input files to the CMAQ. In one pair of simulations, the MODELS-3 preprocessor is allowed to re-diagnose the PBL heights, while for the other pair of simulations, the PBL heights from MM5 are directly imported into the photochemical model. The former simulations will be referred to as BL/MODELS-3 and GS/MODELS-3, while the latter simulations will be referred to as BL/MM5 and GS/MM5. This facilitates a comparison between the effects of the two different PBL schemes on predicted O_3 concentration fields, as well as the effects of different methods of PBL height determination for a given PBL scheme.

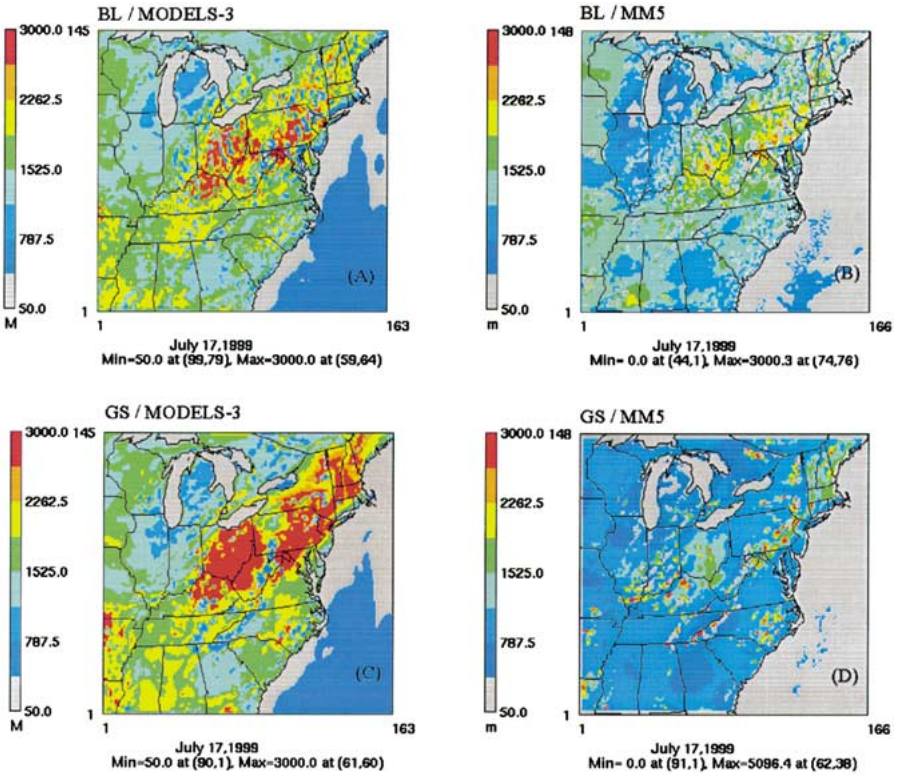

Figure 2. PBL heights at 1800 UTC on July 17 for each of the four base case simulations: (a) BL/MODELS-3; (b) BL/MM5; (c) GS/MODELS-3; (d) GS/MM5.

3. Results and Discussion

3.1. DIFFERENCES IN THE METEOROLOGICAL INPUTS

As noted before, the success of an air quality simulation depends to a large degree on the accuracy of the meteorological fields used as model inputs. Hence, the photochemical model simulations are no more reliable than their respective inputs. Figure 2 displays the calculated PBL heights at 1800 UTC on July 17, 1999 for the four simulations. In general, the bulk Richardson number method used in MODELS-3 yields higher PBL heights than those from MM5 based on either the θ-profile or TKE-profile. The GS/MM5 method generally calculated the lowest PBL heights with isolated pockets of high values in certain geographic areas. Comparing the outputs taken directly from MM5, the BL scheme is more efficient at vertical mixing than the GS scheme, and is able to generate a deeper PBL [10]. On the other hand, in the MODELS-3 re-diagnosis simulations, the GS fields yielded higher PBL heights than those from the BL fields. This result is the opposite of what was predicted by MM5, and is caused by the higher ground temperatures predicted by the GS scheme which strongly affect the bulk Richardson number calculation.

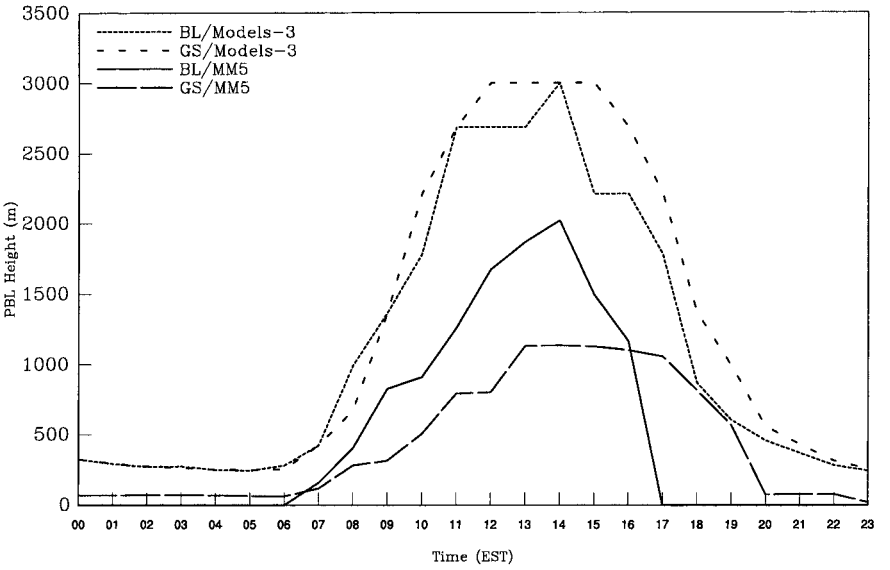

Figure 3. Diurnal variations in the PBL height for each of the four base case simulations at the Baxter site on July 17.

The maximum difference in the mixing heights between the four simulations is on the order of 2 km. These results indicate that substantial uncertainties in the PBL height determination exist due to the differences in the methods of PBL diagnosis and the differences in the meteorological fields.

Figure 3 depicts the diurnal variation of the PBL height for the four simulations at the Baxter site on July 17. The predictions from the MODELS-3 re-diagnoses exhibit a much earlier and dramatic rise, reaching a much higher level than those of the MM5 methods. During the convective daytime hours, the GS/MODELS-3 and BL/MODELS-3 simulations predicted maximum PBL heights of about 3 km. The rapid growth in the PBL height would allow for the entrainment of pollutants trapped aloft, leading to an earlier rise in surface O_3 concentrations; however, the higher PBL height would tend to dilute O_3 and its precursors during the afternoon hours [23, 24]. Comparing with the direct MM5 outputs, the BL version tends to stabilize the PBL earlier than the GS version, causing the earlier and more rapid collapse of the convective boundary-layer.

The simulated cloud cover fractions at 1500 UTC and 2000 UTC re-diagnosed by MODELS-3, representing the sum of the low, middle and high cloud cover fields, are displayed in Figure 4. The GS scheme tends to simulate clearer skies than the BL scheme due to its inability to efficiently transport water vapor from the surface layer to higher levels [10]. Clouds play crucial roles in the transport and removal of pollutants. Firstly, clouds are indicative of the vertical convective transport from the surface to the free troposphere. Secondly, clouds aid in the removal of pollutants via scavenging and wet deposition. Thirdly, clouds can

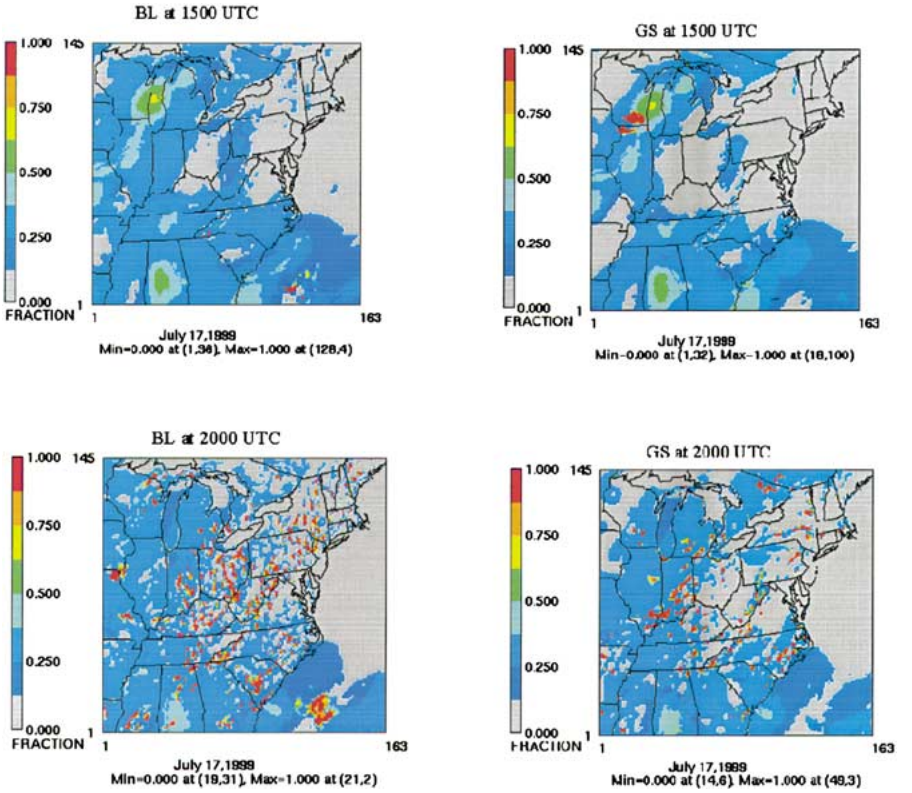

Figure 4. The cloud cover fraction diagnosed by MODELS-3 on July 17 by both PBL schemes. The top two panels are for 1500 UTC, and the bottom two panels are for 2000 UTC.

substantially alter the photolysis rate coefficients. Hence, the CMAQ-predicted O_3 concentrations would be sensitive to the cloud cover simulated by MM5.

The temporal variation in the vertical wind profiles, taken directly from MM5, at the Baxter site on July 17 is depicted in Figure 5. During the morning hours, both schemes simulated similar wind directions, with perhaps slightly higher wind speeds in the lower levels predicted in the BL simulation. Above about 1.3 km AGL, the wind direction changed from southwesterly into westerly. Figure 5 indicates that the wind fields simulated by the two PBL schemes deviated during the onset of the convective boundary-layer; the GS version simulated more southwesterly flow while the BL version simulated more southerly flow during the daytime convective periods. At the onset of convective conditions, the BL scheme quickly brings the surface momentum flux to higher layers, with more southerly flow and higher wind speeds from about 1400–1800 EST, while the GS scheme still maintains southwesterly flow. During the daytime periods, the wind direction further changes from westerly to northwesterly above about 1.7 km AGL. This is more consistent with the PBL height diagnosed in the MM5 simulations with the BL scheme than the GS scheme [10]. As a result of these wind field differences,

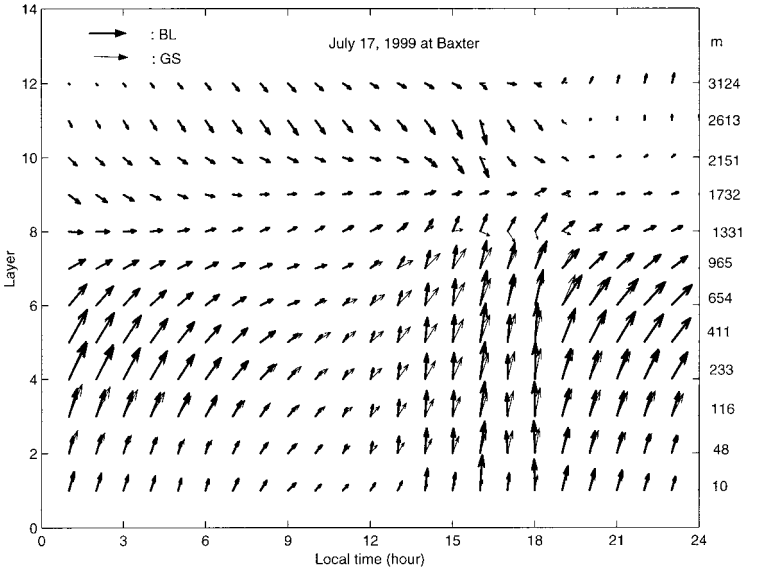

Figure 5. Time series of wind profiles at the grid cell corresponding to the Baxter site on July 17 from both PBL schemes, extracted directly from MM5. Both the model level and the approximate height AGL are shown.

pollutants and precursors will be transported along different directions in the model simulations, contributing to differences in the predicted O_3 concentration fields.

The above analysis is limited to one grid cell. To illustrate the behavior of the BL and GS wind fields spatially, Figure 6 depicts the wind fields in the analysis subdomain at 2000 UTC on July 17. Large differences between the two simulations occur along the coast of New Jersey and near Long Island. In these regions, the BL simulation predicted a stronger sea breeze than the GS simulation due to the more vigorous vertical mixing of the BL version, which maintained a much deeper layer of temperature contrast between land and ocean than that of the GS scheme [10, 22].

3.2. COMPARISON BETWEEN O_3 MODEL SIMULATIONS

3.2.1. *Spatial Pattern of Maximum of Hourly O_3 Concentrations*

The model-predicted daily maximum surface O_3 concentrations at each grid cell over the analysis subdomain for the four simulations on July 17 are presented in Figure 7. The GS versions (Figures 7b and 7e) generally simulated higher surface 1-h O_3 concentrations than the BL versions (Figures 7a and 7d); the corresponding model-to-model differences (expressed in percent) appear in the panels of Figures 7c and 7f. The differences in the vertical mixing processes as well as transport within the PBL can contribute to the differences in the formation and accumulation of O_3 concentrations; for the MODELS-3 re-diagnoses (Figures 7a and 7b), the GS

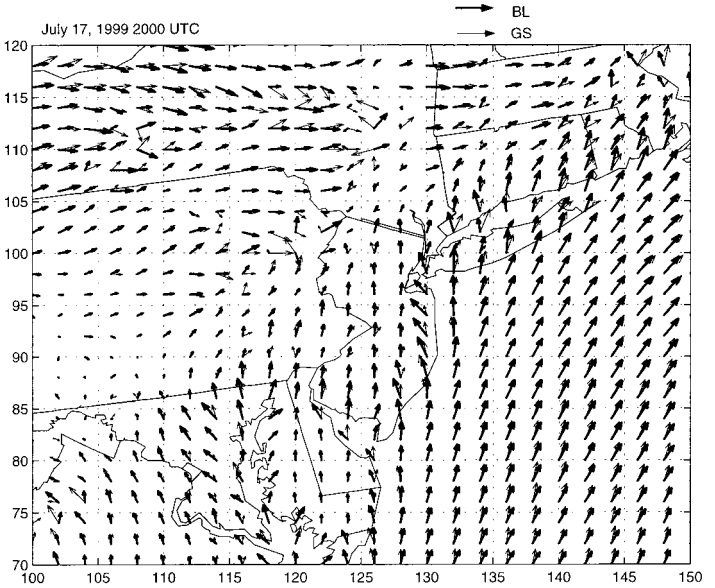

Figure 6. Near-surface wind fields predicted by both PBL schemes on July 17 at 2000 UTC within the analysis subdomain, extracted directly from MM5.

simulated the peak in the Connecticut area, while the BL simulated the peak in the southeastern Pennsylvania area. The BL/MODELS-3 and GS/MODELS-3 simulations predicted only small isolated regions of daily maximum O_3 concentrations above 120 ppb. However, the daily 1-h maximum O_3 patterns are qualitatively similar. The differences in the locations of the simulated peak concentrations are mostly due to the differences in the wind fields, more southwesterly in the GS version and more southerly in the BL version, especially during the daytime convective periods.

The impact of the PBL schemes on O_3 simulations is moderated considerably by the MODELS-3 re-diagnosis of PBL heights (Figures 7a and 7b) compare with (Figures 7d and 7e), which reflect the simulations when the MM5 PBL heights are directly imported. The BL/MM5 simulated large areas of daily maximum O_3 concentrations between 120–140 ppb along the urban corridor, while the GS/MM5 simulated large regions in excess of 140 ppb. When the MM5 outputs are used directly, it is evident from Figures 7c and 7f that the differences between the simulated daily maximum surface O_3 concentrations are substantial, with the GS simulations 30–40% higher than the corresponding BL simulations along the coast and urban corridor, indicating the strong sensitivity of the simulated O_3 to the PBL scheme employed. The large differences between the BL/MM5 and GS/MM5 simulations, especially along the Atlantic coast, may be due to the higher PBL heights and stronger sea breeze circulation in the BL scheme. However, in the MODELS-3 re-diagnosis simulations, the differences between the BL and GS simulations are generally within $\pm 10\%$ along the urban corridor, with the largest differences ($>$10–20%) mostly confined to the Delmarva peninsula.

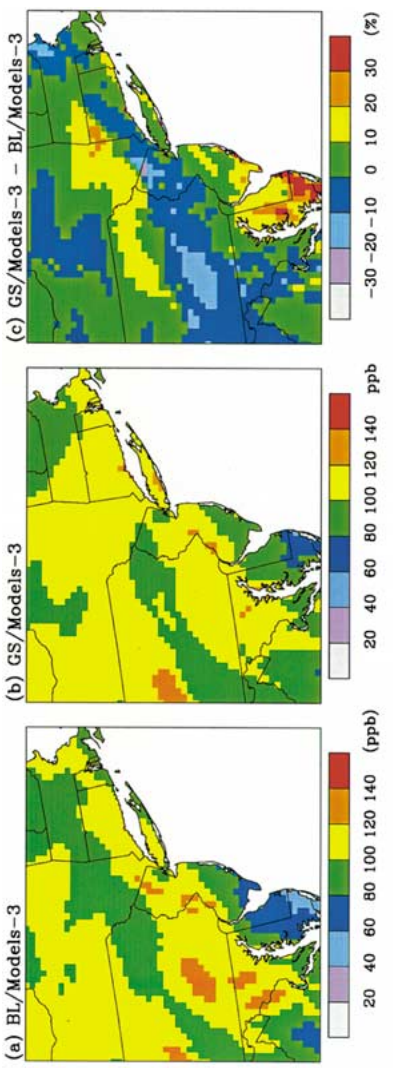

Figure 7. Spatial map of predicted maximum 1-h O_3 concentration on July 17. The top row of panels indicate the simulations in which MODELS-3 re-diagnosed the PBL heights, while the bottom row indicates the simulations in which the PBL heights were taken directly from MM5. The leftmost panels are the BL simulations, the middle panels are the GS simulations, and the rightmost panels show the respective differences ('BL minus GS').

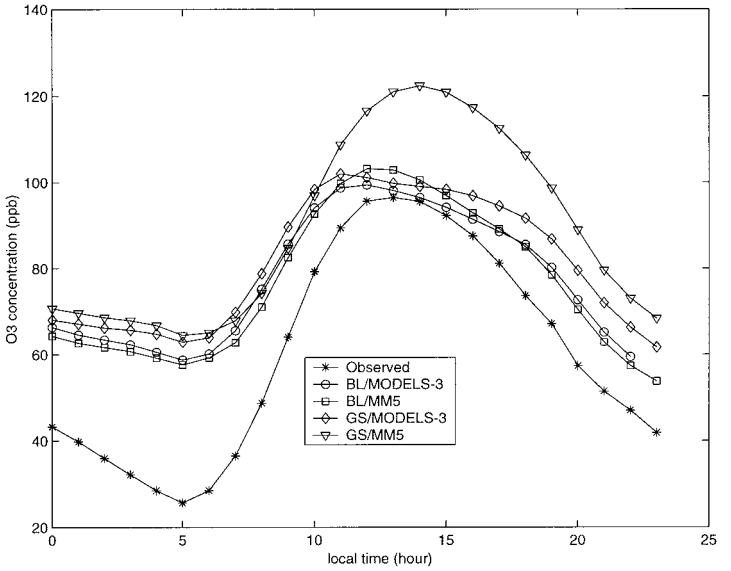

Figure 8. Observed and predicted O_3 concentrations on July 17, for each of the four base case simulations. Data from all 118 monitoring sites within the analysis subdomain were averaged here.

During the period of July 15–19, 1999, the eastern United States was under the influence of a high-pressure system. The weather conditions for this episode are characterized by high temperatures, strong shortwave radiation, low wind speeds, and low inversion heights [10]. The GS/MM5 scheme simulated higher surface temperatures, lower wind speeds during the morning hours, and less cloud cover than the BL/MM5 scheme, but the simulated PBL heights were too low. The BL/MM5 scheme diagnosed the PBL height comparable to the observed values [10], but the strong vertical mixing may alter the surface wind direction too much. Furthermore, the overestimated PBL heights by the MODELS-3 re-diagnosis tend to dilute the O_3 concentrations and smear out some of the differences between the GS and BL schemes. Observations, having adequate spatial and temporal resolution over the diurnal cycle are, therefore, needed to properly evaluate these models in light of the existing uncertainties.

3.2.2. *Diurnal Behavior of Simulated O_3*

Figure 8 depicts the diurnal variations in the observed and predicted O_3 concentrations on July 17, averaged over all grids in the analysis subdomain, for each of the four base case simulations. From midnight until early morning, all four simulations significantly overpredicted the observed O_3 concentrations; these overpredictions may be attributable to the vertical eddy diffusivity in the surface layer and inadequate treatment of pollutant removal processes in the model's first layer. In the CMAQ, the vertical diffusivity in the surface layer is assigned a fixed minimum

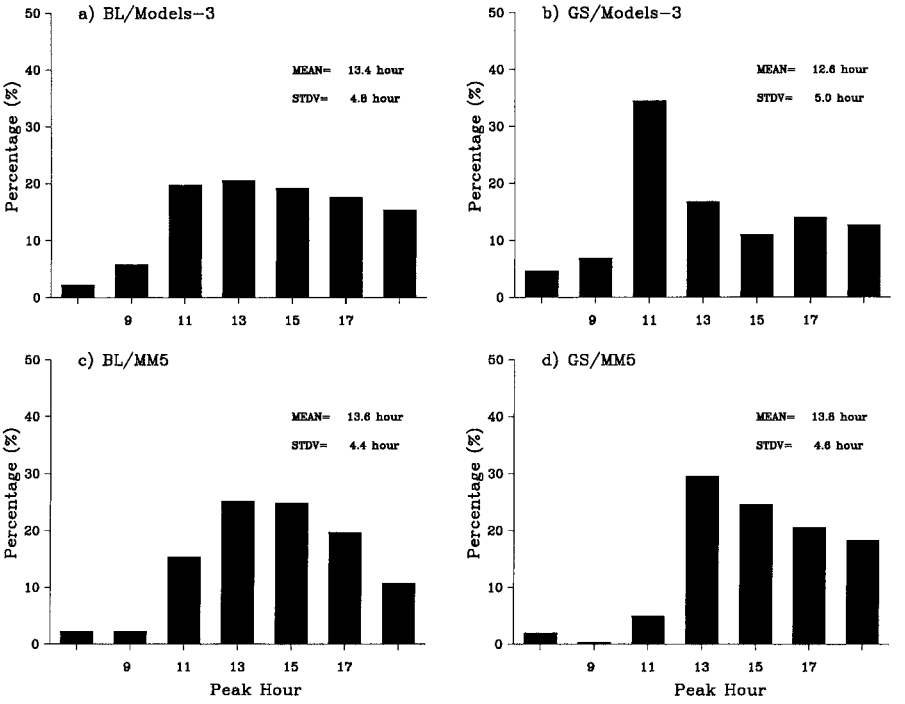

Figure 9. Histograms of the time of occurrence of the 1-h maximum O_3 concentrations, for each of the four base case simulations on July 17: (a) BL/MODELS-3; (b) BL/MM5; (c) GS/MODELS-3; (d) GS/MM5.

value of 1 m^2 s^{-1}. Although CMAQ started with higher O_3 concentrations than those observed, the model seems to reproduce the observed 1-h O_3 concentration peak in the afternoon hours reasonably well, except for the GS/MM5 case. The BL cases are more consistent with each other, generally capturing the observed peak on average. Also, the GS simulations are very different from each other during the convective time periods (see Figure 8). While the GS/MODELS-3 simulation predicted an average peak concentration of about 120 ppb, the observations and the other three simulations only reached about 100 ppb for the average daily maximum concentration. Note the simulations with overestimated PBL heights from the MODELS-3 re-diagnosis tend to predict peaks earlier in time than those of lower PBL heights provided by MM5.

The histograms of the time of occurrence of the simulated daily maximum 1-h O_3 concentrations on July 17 are presented in Figure 9. In general, both BL and GS schemes with PBL heights diagnosed by MM5 (BL/MM5 and GS/MM5 cases) tended to simulate the timing of the daily peaks around 1300 and 1500 EST. The GS/MODELS-3 case simulated an earlier peak around 1100 EST, while the BL/MODELS-3 case simulated the peak at 1300 EST. With the MODELS-3 re-diagnosis of the PBL heights (BL/MODELS-3 and GS/MODELS-3), the dynami-

cal balance from MM5 is altered; MODELS-3 diagnosed the PBL heights as high as 3 km during the daytime convective period, but the PBL height diagnosis based upon both observations and MM5 predictions of temperature and wind profiles do not indicate that the PBL is this deep [10]. The MODELS-3 re-diagnosis estimates much higher PBL heights and an earlier rise in PBL evolution than does MM5. Hence, it is important to insure dynamical consistency of the meteorological fields in the air quality model to properly simulate the pollutant dynamics within the boundary-layer.

To illustrate the effects of different vertical mixing mechanisms on the diurnal evolution of the O_3 concentrations, the time-height cross-sections of O_3 on July 17 at the Baxter site are displayed in Figure 10 for each of the four simulations. In CMAQ, the vertical diffusion is parameterized by the K-theory. The convective vertical diffusivity is calculated as a function of surface heat flux and the PBL height. The stronger vertical diffusion in the MODELS-3 re-diagnosed simulations leads to the deeper PBL heights, allowing high winds aloft to transport pollutants farther downwind from the source region. Note the presence of very high O_3 concentrations aloft ($>$120 ppb) in the re-diagnosed simulations near 2 km, which persist throughout the second half of the day. Comparing the BL/MM5 and GS/MM5 simulations, the earlier collapse of the mixed layer of the BL scheme depletes the surface O_3 level much earlier than the GS scheme. The GS/MM5 simulation, having the weakest vertical diffusion, predicts very stratified O_3 concentrations throughout much of the day, and permits high concentrations ($>$110 ppb) to be trapped below about 1 km with much lower O_3 levels aloft then BL/MM5. This will certainly have an impact on the predicted surface concentrations farther downwind of the source region on the following day.

The scatter plots of the predicted daily maximum 1-h O_3 concentrations at each grid cell within the analysis subdomain are depicted in Figure 11 for the four simulations, along with the least-squares fit line on July 17. Figure 11a displays the comparison between the two BL simulations. The correlation coefficient of 0.93 indicates that there is similar performance between the two BL simulations, estimated either from the bulk Richardson number or the θ-profile. A large difference occurs in the performance between the two GS simulations (see Figure 11b). The difference is mainly caused by the large discrepancy in the PBL height, since the same meteorological fields were used in both simulations; the lower PBL height estimated by TKE-profile method resulted in much higher predicted surface O_3 concentrations than in the MODELS-3 re-diagnosis simulation. The correlation is the lowest of the four comparisons in Figure 11. Figures 11c and 11d display the effects of the different PBL schemes on O_3 simulations. The correlation coefficients in Figures 11c and 11d are higher than in Figure 11b, since the differences between the two BL and GS schemes for a given method of PBL diagnosis are smaller than the differences between the MODELS-3 and MM5 methods associated with the GS scheme.

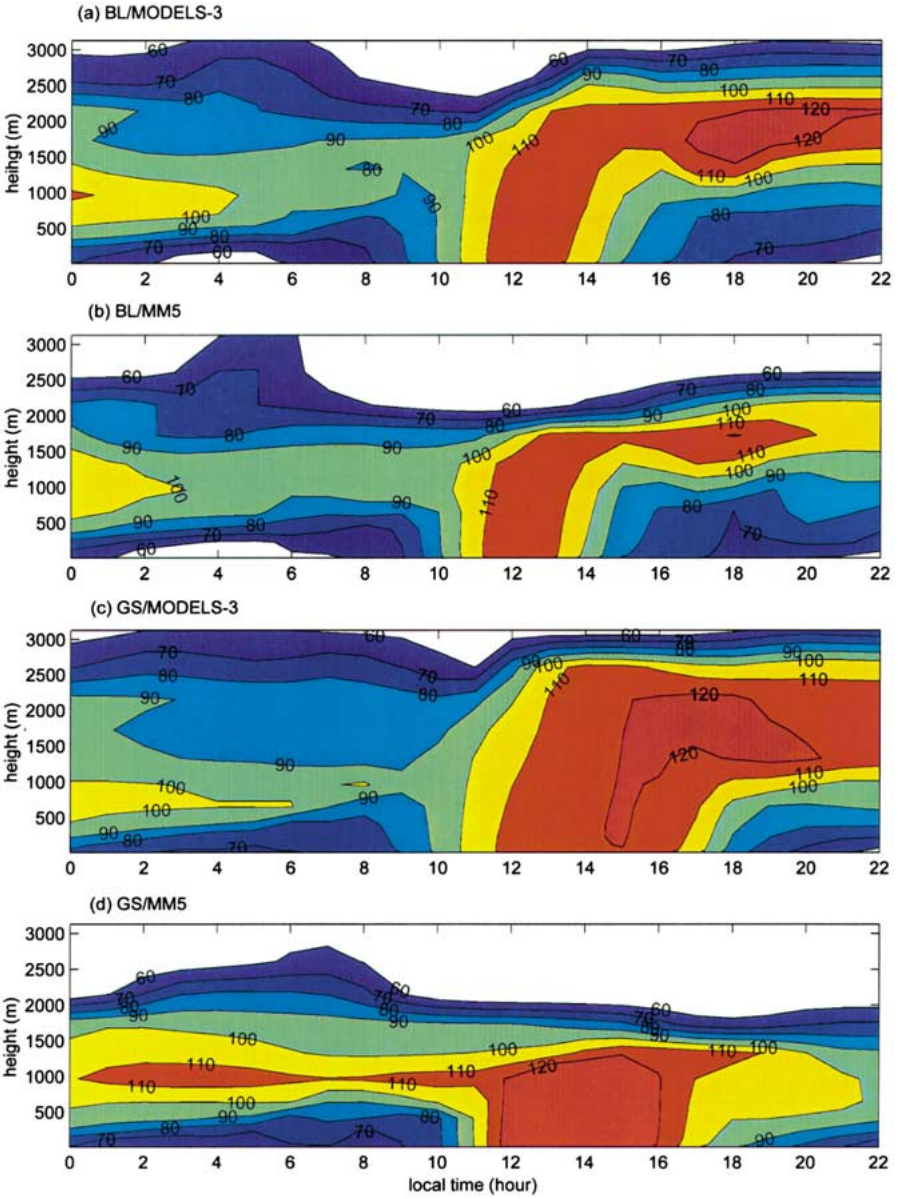

Figure 10. Time-height cross section of O_3 concentrations at the Baxter site on July 17, for each of the four base case simulations: (a) BL/MODELS-3; (b) BL/MM5; (c) GS/MODELS-3; (d) GS/MM5.

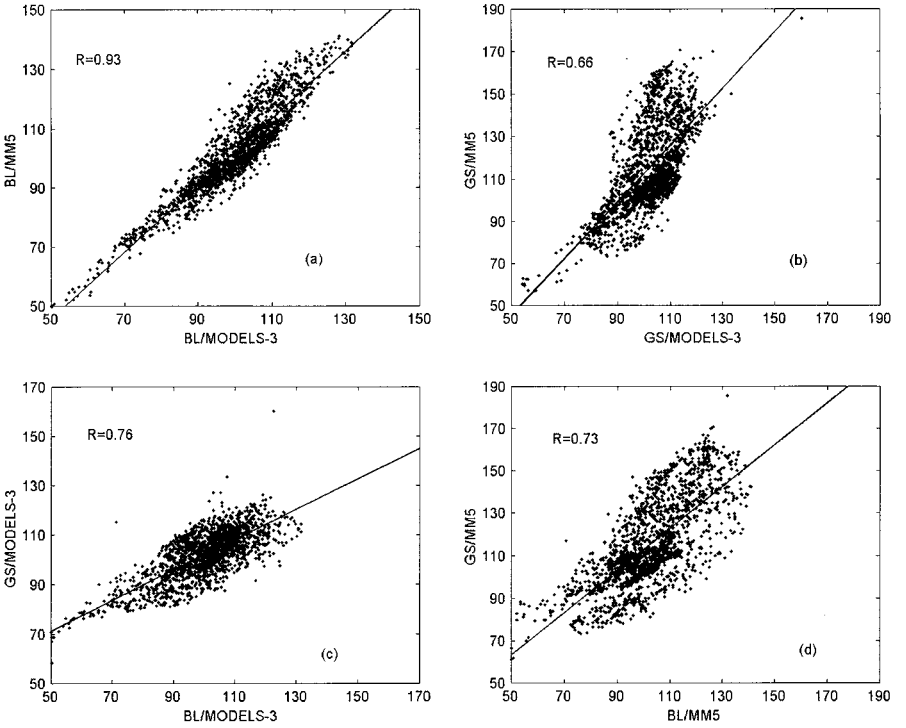

Figure 11. Scatter plots of the predicted daily maximum 1-h O_3 concentrations on July 17: (a) BL/MM5 versus BL/MODELS-3; (b) GS/MM5 versus GS/MODELS-3; (c) GS/MODELS-3 versus BL/MODELS-3; (d) GS/MM5 versus BL/MM5.

3.3. PROCESS ANALYSIS

To examine the importance of the different physical and chemical processes that lead to the formation, distribution, and destruction of O_3 in the CMAQ simulations, we applied process analysis (PA) to quantify the relative contributions of individual processes. Figure 12 shows the temporal variation of the contributions based on the values at the model's second layer (about 50 m AGL) from four processes – chemical reactions, vertical diffusion, cloud effects and horizontal advection – averaged over the analysis domain for the four simulations. The two re-diagnosed simulations, BL/MODELS-3 and GS/MODELS-3, had smaller contributions from chemical formation, which may be due to the higher PBL heights diagnosed with the MODELS-3 preprocessor, leading to higher dilution of O_3 and precursor concentrations during the daytime convective period. These two simulations also predicted an earlier rise in the PBL, evident in the important contributions of vertical diffusion from 0700–0900 EST to O_3 formation. The GS/MM5 simulation predicted the shallowest PBL heights, the largest contributions from chemical reactions (O_3 formation), and the largest contributions from horizontal advection (O_3 destruction) during the daytime.

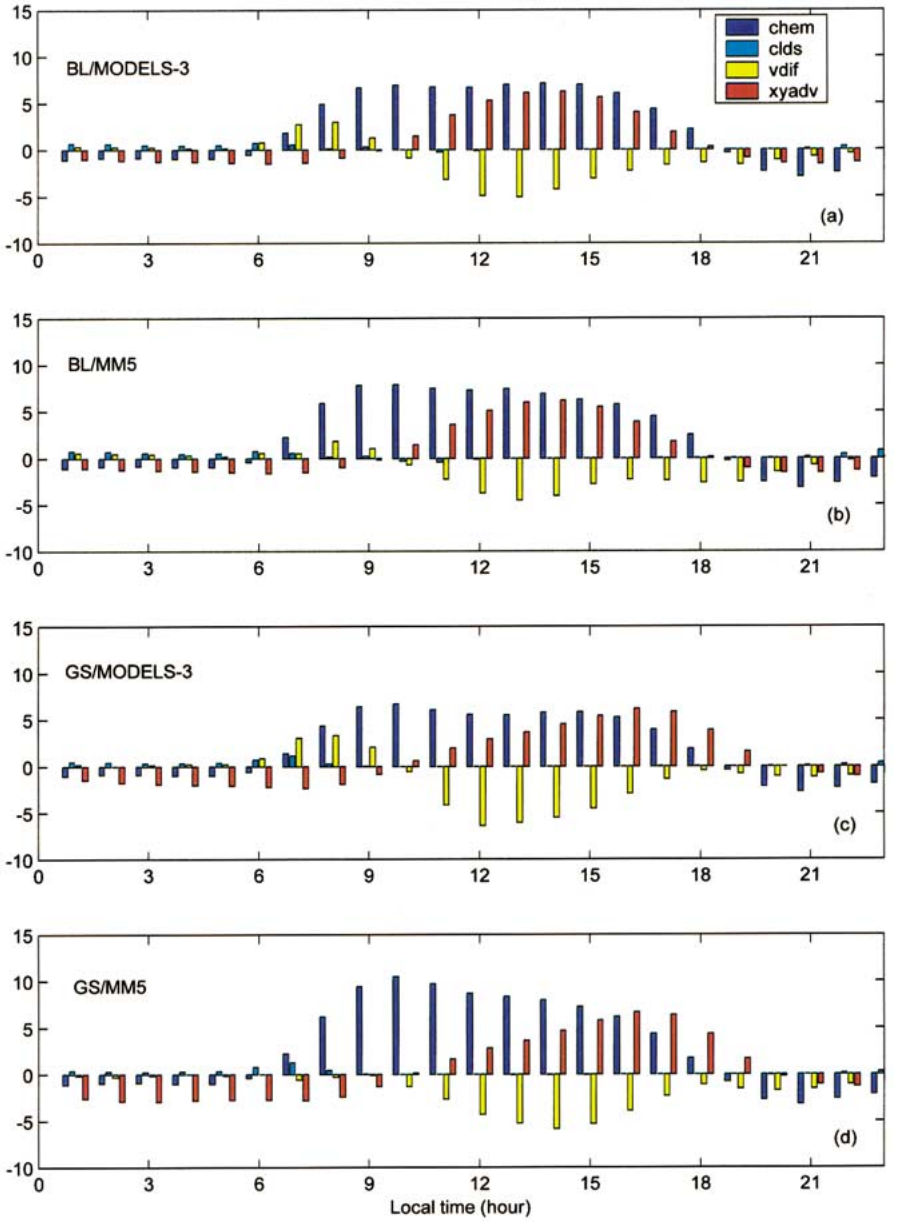

Figure 12. Time series of the relative contributions of chemical reactions, vertical diffusion, and horizontal advection, for each of the four base case simulations: (a) BL/MODELS-3; (b) BL/MM5; (c) GS/MODELS-3; (d) GS/MM5.

Table I. Predicted daily 1-h maximum ozone concentration (ppb) on July 15, 1999, for the base case and two emissions control cases. The two control cases refer to different amounts of anthropogenic emissions reductions: *N50V25* = 50% NO_x reduction, 25% VOC reduction; *N25V50* = 25% NO_x reduction, 50% VOC reduction.

	Base case (ppb)	N50V25 case (ppb)	N25V50 case (ppb)
BL/MODELS-3	118	96	107
BL/MM5	125	99	111
GS/MODELS-3	138	148	135
GS/MM5	145	157	133

Note that throughout the day, the differences between the two BL simulations are smaller than the differences between the two GS simulations, both in terms of the magnitudes and diurnal variations of the individual contributions. This is not surprising, since the differences in simulated PBL evolution and heights are smaller between the BL simulations. During the daytime, the largest O_3 destruction rates due to vertical diffusion are about -5 ppb h^{-1} ($\sim$1400 EST) for the GS/MM5 case while the highest formation rates due to chemical reactions, nearly 10 ppb h^{-1}, occur from 0900 to 1100 EST. The largest contributions to O_3formation from horizontal advection occur between 1500 and 1700 EST. For the GS/MODELS-3 case, only the afternoon loss rate due to horizontal advection is similar to the GS/MM5 case, while the morning formation rates from chemical reactions are lower; however, the loss rate due to vertical diffusion is substantial from 1200 to 1500 EST, with the maximum contribution shifted two hours earlier.

3.4. RESPONSE OF O_3 SIMULATIONS TO EMISSION REDUCTIONS

Table I lists the predicted maximum 1-h O_3 concentrations on July 15 over the analysis subdomain for each of the base cases, and the corresponding anthropogenic emission reduction scenarios – NO_x-focused (N50V25) controls and VOC-focused (N25V50) controls. Although the O_3 episode was only beginning in the northeastern U.S. on July 15, we chose this day to illustrate the sensitivity of the CMAQ to different emissions reduction cases. Table I indicates that the GS scheme simulated higher 1-h daily O_3 maxima than the BL scheme over the analysis subdomain. Also, the NO_x-focused controls are more effective in reducing the domain-wide maximum in the BL simulations when compared with the GS simulations; the NO_x-focused control scenario actually led to an increase in the peak 1-h O_3 over the New York City area for the GS case, due to the reduced NO scavenging. Also, the NO_x-focused controls were more effective than the VOC-focused controls in reducing O_3 in the BL simulations. The responses of the emission changes

are greater in the MM5 PBL hight cases than the MODELS-3 PBL height cases in both the BL and GS PBL schemes.

While Table I only reflects the changes in the daily maximum O_3 occurring at any grid cell within the analysis subdomain, it is important to examine the overall spatial patterns in the model predictions. The relative response of the model to the different emission reduction scenarios is defined in terms of the index of improvement:

$$\text{Index of improvement} = \frac{(O_3)_{\text{base}} - (O_3)_{\text{control}}}{(O_3)_{\text{base}}} \times 100\%. \quad (1)$$

Figure 13 (MODELS-3 PBL height cases) and 14 (MM5 PBL height cases) display the index of improvement for 1-h O_3 concentrations for the VOC-focused controls and the NO_x-focused scenarios as difference plots, defined as 'BL minus GS', for all of the four simulations.

The NO_x-focused controls show an overall larger index of improvement than the VOC-focused controls with both PBL schemes, although the effects of the reduced NO scavenging (resulting in O_3 increases from the base case) are evident in the vicinity of and downwind of the New York City metropolitan area. Note the different scales in Figures 13 and 14 for the two emissions reduction scenarios. Qualitatively, for a given emissions control scenario, the overall patterns for the index of improvement are similar for the cases of MODELS-3 PBL heights (Figure 13), while they show significant differences for the MM5 PBL height cases (Figure 14) over much of the domain. The differences between the BL and GS schemes are within $\pm 5\%$ for the N50V25 scenario, and within $\pm 2.5\%$ for the N25V50 scenario in the cases of MODELS-3 processed PBL height cases (Figure 13). These differences are doubled in the MM5 PBL height cases (Figure 14). For the NO_x-focused control, there are large differences in complex geographical areas such as the Long Island Sound area, where the BL scheme predicted indexes of improvement which were about 10–20% lower than those predicted by the GS scheme. This is not unexpected, since the PBL processes can substantially alter the meteorological fields on the smaller scale. Also, significant differences are evident in the Catskills and Hudson Valley regions of New York State, where the BL scheme predicted indexes of improvement which were about 5–15% higher than in the GS scheme. For the VOC-focused control case, the differences in the index of improvement simulated by the two PBL schemes were always within $\pm 10\%$ across the entire analysis subdomain.

The uncertainty in the estimation of PBL heights will influence the model's response to emission reductions. The higher ventilation in the BL case tends to favor NO_x reductions over VOC reductions; when the morning time ventilation is high (i.e., high mixing height and/or high wind speed), freshly injected NO emissions tend to be dispersed so that reductions in NO_x emissions lead to a greater reduction in the daily maximum 1-h O_3 concentration; on the other hand, when the morning time ventilation is low (i.e., low mixing height and/or low wind speed), freshly

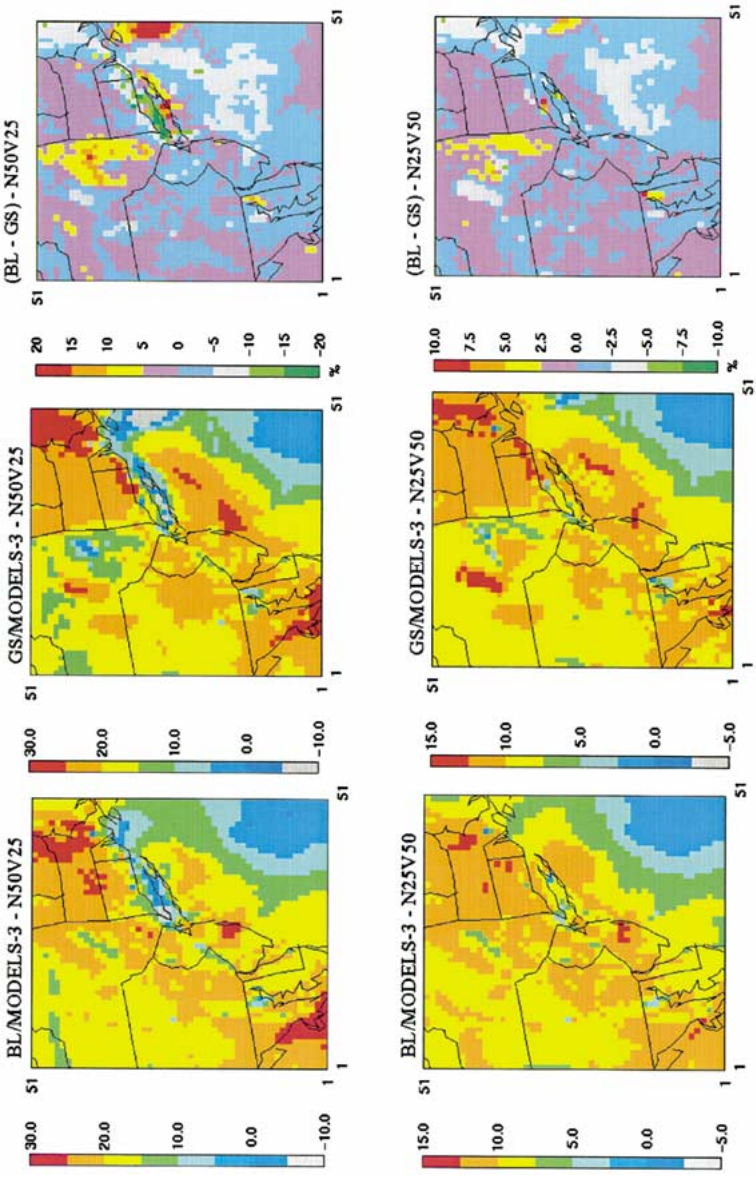

Figure 13. The differences ('BL minus GS') in the index of improvement of daily maximum 1-h O_3 concentrations, for the MODELS-3 re-diagnosed simulations. The two emissions control scenarios are NO_x-focused (NO_x reduced by 50% and VOC reduced by 25% denoted as N50V25) or VOC-focused (NO_x reduced by 25% and VOC reduced by 50% denoted as N25V50). The left panel corresponds to the N50V25 case, and the right panel corresponds to the N25V50 case.

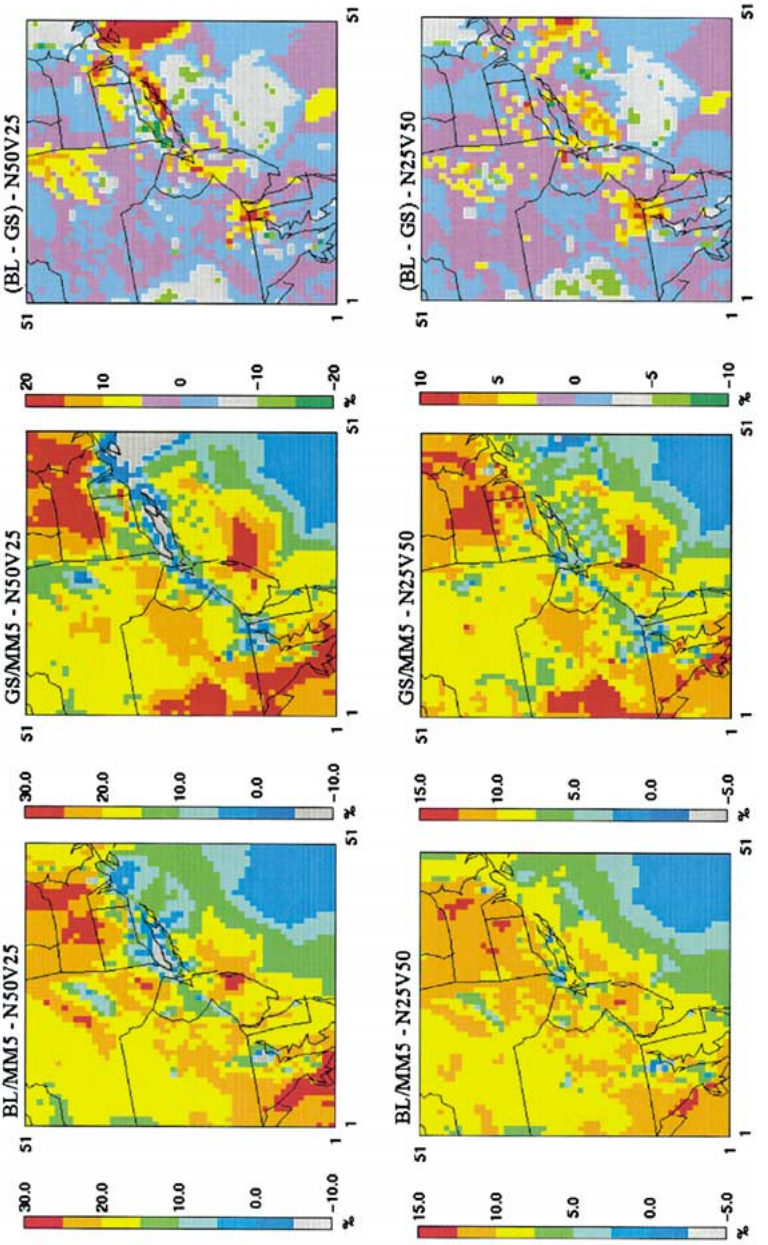

Figure 14. Same as Figure 13, except for the MM5 PBL heights simulations.

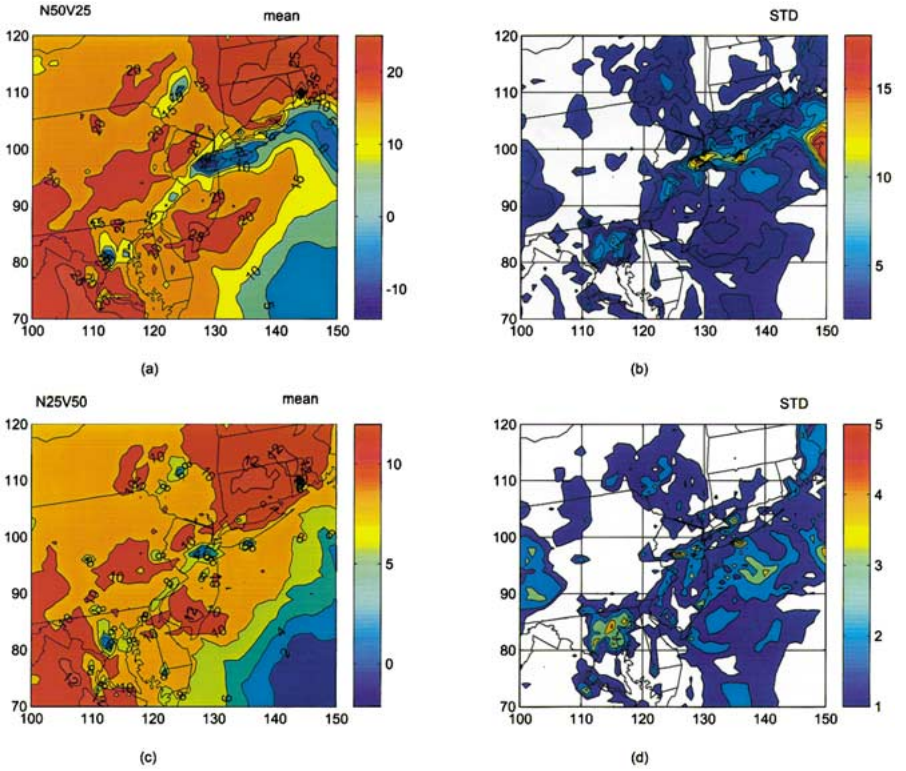

Figure 15. Mean and standard deviation of the index of improvement from all four simulations for the NO_x-focused and VOC-focused control cases.

injected NO emissions lead to NO titration so that reductions in NO_x emissions can actually increase the daily maximum O_3 concentration [24]. As stated earlier, the MODELS-3 pre-processor tends to reduce the differences between the two PBL schemes at the expense of internal consistency. When the index of improvement with same the PBL scheme but different PBL height diagnosis (i.e., BL/MODELS-3 vs BL/MM5, or GS/MODELS-3 vs GS/MM5) are plotted against each other (not shown here), they are highly correlated with each other in the BL cases but not in the GS cases. In the lower PBL height cases of GS/MM5, they increase the areas of greater benefit from both NO_x and VOC reduction cases when compared to GS/MODELS-3, and they also increase the areas with negative benefits, especially near the source areas.

The uncertainty of the meteorological inputs caused the deviations in the simulated index of improvement from the emission reductions. It is of interesting to investigate the 'ensemble' of all simulations. Figure 15 shows the mean and standard deviation of index of improvement from all four simulations for the NO_x-focused and VOC-focused controls. The mean values of the index of improvement for the NO_x-focused case (Figure 15a) range between -15% to 25%, with larger

negative values located in New York City and downwind. The standard deviations (Figure 15b) are also very high in those areas. The VOC-focused cases (Figures 15c and 15d) show similar results with smaller range of the mean and standard deviation. Although only four cases of PBL treatment are considered here, the simulated results illustrate the potential for a large uncertainty in the efficacy of NO_x controls in the areas often associated with high O_3 concentrations (for example, New York City and downwind), due to the complex emissions pattens and geographic features (e.g., land-water). Therefore, it is important to have observations of the PBL evolution to validate the PBL schemes used in the meteorological model if we are to reduce these uncertainties.

4. Summary

In this paper, we examined the uncertainties in air quality modeling stemming from the differences in the PBL schemes considered in the meteorological model. The different methods of treating subgrid-scale vertical mixing processes in MM5 would result in different vertical profiles of temperature, cloud cover, and winds. The uncertainties in the meteorological parameters will, in turn, propagate through the photochemical model simulations. The modeling results presented in this study demonstrate that the differences in the predicted peak O_3 concentrations can be as high as 40 ppb. In addition to the differences in the magnitudes of peak predicted O_3, the time of occurrence of peak O_3 concentrations at a given grid cell or region can differ by several hours. Thus, the predictions of absolute levels of daily maximum 1-h O_3 concentrations at individual grid cells on individual days by the current generation of photochemical modeling systems will be highly uncertain.

To date, episodic air quality modeling studies have been performed in a deterministic sense in the regulatory setting using certain choices of the model physics and data [25]. In reality, it is impossible to exhaust all possible combinations of the air quality modeling system, which couple the meteorological model and photochemical model. It is essential to characterize the uncertainty in the modeling results due to the choices of equally valid sources of data and model physics. In this study, we demonstrated the importance of the PBL height, which defines the vertical extent of the well-mixed layer on the results of the air quality simulation. To reduce the uncertainty caused by errors in the PBL height, a more realistic formulation for the PBL height – requiring observations having a high degree of temporal, horizontal, and vertical resolution – is essential for photochemical modeling. The proper dynamical balance of the meteorological fields is needed to provide the air quality model with the correct physical processes in simulating the behavior of the pollutants within the boundary-layer. It is, therefore, essential that the pre-processor of the air quality model not alter the outputs of the meteorological model.

Acknowledgements

This work was supported in part by the New York State Energy Research and Development Authority (NYSERDA) under agreement numbers 4914-ERTER-ES99 and 6085-ERTER-ES00, the U.S. EPA under grant number R826731476, and the New York State Department of Environmental Conservation (DEC). The views expressed in this paper do not necessarily reflect those of the supporting agencies.

References

1. Seaman N.L.: 2000, Meteorological modeling for air-quality assessments, *Atmos. Environ.* **34**, 2231–2259.
2. Biswas, J. and Rao, S.T.: 2001, Uncertainties in episodic ozone modeling stemming from uncertainties in the meteorological fields, *J. Appl. Meteorol.* **40**, 117–136.
3. Sistla, G., Hao, W., Ku, J.Y., Kallos, G., Zhang, K., Mao, H. and Rao, S.T.: 2001, An operational evaluation of two regional-scale ozone air quality modeling systems over the eastern United States, *Bull. Amer. Meteorol. Soc.* **82**, 945–964.
4. Alapaty, K., Olerud, D.T., Schere, K. and Hanna, A.F.: 1995, Sensitivity of regional oxidant model predictions to prognostic meteorological fields, *J. Appl. Meteorol.* **34**, 1788–1801.
5. Lorenz, E.N.: 1963, Deterministic nonperiodic flow, *J. Atmos. Sci.* **20**, 130–141.
6. Russell, A. and Dennis, R.: 2000, NARSTO critical review of photochemical models and modeling, *Atmos. Environ.* **34**, 2283–2324.
7. Rao, S.T., Ku, J.Y., Berman, S., Zhang, K. and Mao, H.: 2001, Summertime characteristics of the atmospheric boundary-layer and relationships to ozone levels over the eastern U.S., *Pure Appl. Geophys*, in press.
8. Alapaty K., Pleim, J., Raman, S., Niyogi, D.S. and Byun, D.W.: 1997, Simulation of atmospheric boundary processes using local- and nonlocal-closure schemes, *J. Appl. Meteorol.* **36**, 214–233.
9. Berman S., Ku, J.Y. and Rao, S.T.: 1999, Spatial and temporal variation of the mixing depth over the northeastern United States during the summer of 1995, *J. Appl. Meteorol*. **38**, 1661–1673.
10. Zhang, K., Mao, H., Civerolo, K., Berman, S., Ku, J.-Y., Rao, S.T., Doddridge, B., Philbrick, C.R. and Clark, R.: 2001, Numerical investigation of boundary layer evolution and nocturnal low-level jets: local versus non-local PBL schemes, *Environ. Fluid Mech.* **1**, 171–208.
11. Alapaty K. and Mathur, R.: 1998, Effects of boundary layer mixing representations on vertical distribution of passive and reactive tracers, *Meteorol. Atmos. Phys.* **69**, 101–118.
12. Hogrefe, C., Rao, S.T., Kasibhatla, P., Kallos, G., Tremback, C.J., Hao, W., Olerud, D., Xiu, A., McHenry, J. and Alapaty, K.: 2001, Evaluating the performance of regional-scale photochemical modeling systems: part 1 – meteorological predictions, *Atmos. Environ.* **35**, 4159–4174.
13. Rao, S.T., Sistla, G., Ku, J.Y., Zhou, N. and Hao, W.: 1994, Sensitivity of the Urban Airshed Model to mixing height profile. In: *Proceedings of the Eighth AMS/AWMA Joint Conference on the Applications of Air Pollution Meteorology*, Nashville, TN.
14. Sistla, G., Zhou, N., Hao, W., Ku, J.Y., Rao, S.T., Bornstein, R., Freedman, F. and Thunis, P.: 1996, Effects of uncertainties in meteorological inputs on urban airshed model predictions and ozone control strategies, *Atmos. Environ.* **30**, 2011– 2025.
15. Dudhia, J.: 1993, A nonhydrostatic version of the Penn State-NCAR mesoscale model: validation tests and simulation of an Atlantic cyclone and cold front, *J. Appl. Meteorol.* **121**, 1493–1513.

16. Blackadar, A.K.: 1979, High resolution models of the planetary boundary layer. In: J. Pfafflin and E. Ziegler (eds.), *Advances in Environmental Science and Engineering*, Vol. 1, No. 1, pp. 50–85, Gordon and Breach.
17. Gayno, G.A., Seaman, N.L., Lario, A.M. and Stauffer, D.R.: 1994, Forecasting visibility using a 1.5-order closure boundary layer scheme in a 12-km non-hydrostatic model. In: *AMS Tenth Conference on Numerical Weather Prediction*, pp. 18–20, Portland, OR.
18. Byun, D.W. and Ching, J.K.S.: 1999, *Science Algorithms of the EPA MODELS-3 Community Multiscale Air Quality (MODELS-3) Modeling System*, Report EPA/600/R-99/030, Environmental Protection Agency, Research Triangle Park, NC.
19. Philbrick, C.R.: 1998, Investigations of factors determining the occurrence of ozone and fine particles in northeastern U.S.A. In: *Measurement of Toxic and Related Air Pollutants*, pp. 248–260, Air & Waste Management Association and the U.S. EPA's National Exposure Research Laboratory, Cary, NC.
20. Zhang, D. and Anthes, R.A.: 1982, A high-resolution model of the planetary boundary layer – sensitivity tests and comparisons with SESAME-79 data, *J. Appl. Meteorol.* **21**, 1594–1609.
21. Gery, M.W., Whitten, G.Z., Killus, J.P. and Dodge, M.C.: 1989, A photochemical kinetics mechanism for urban and regional scale computer modeling, *J. Geophys. Res.* **94**, 12925–12956.
22. Shafran, P.C., Seaman, N.L. and Gayno, G.A.: 2000, Evaluation of numerical predictions of boundary layer structure during the Lake Michigan ozone study, *J. Appl. Meteorol.* **39**, 412–426.
23. Zhang, J. and Rao, S.T.: 1999, The role of vertical mixing in the temporal evolution of ground-level ozone concentrations, *J. Appl. Meteorol.* **38**, 1674–1691.
24. National Research Council (NRC): 1999, Ozone photochemistry. In: *Ozone-Forming Potential of Reformulated Gasoline*, pp. 23–32, National Academy Press, Washington, DC.
25. Environmental Protection Agency (EPA): 1991, *Guideline for Regulatory Application of the Urban Airshed Model*, Report EPA-450/4-91-013, Environmental Protection Agency, Research Triangle Park, NC.